Drainage on a rough surface

2011 EPL 94 16002

(http://iopscience.iop.org/0295-5075/94/1/16002)

epl A Letters Journal Exploring the Frontiers of Physics

April 2011

EPL, **94** (2011) 16002
doi: 10.1209/0295-5075/94/16002

www.epljournal.org

Drainage on a rough surface

J. Seiwert[1,2], M. Maleki[3], C. Clanet[1,2] and D. Quéré[1,2(a)]

[1] *Physique et Mécanique des Milieux Hétérogènes, UMR 7636 du CNRS, ESPCI - 75005 Paris, France, EU*
[2] *Ladhyx, UMR 7646 du CNRS, École Polytechnique - 91128 Palaiseau Cedex, France, EU*
[3] *Institute for Advanced Studies in Basic Sciences - P.O. Box 45195-1159, Zanjan 45137-66731, Iran*

received 31 January 2011; accepted in final form 7 March 2011
published online 7 April 2011

PACS 68.15.+e – Liquid thin films
PACS 47.85.mf – Lubrication flows
PACS 47.55.nb – Capillary and thermocapillary flows

Abstract – We discuss the drainage of a wetting film deposited on a vertical solid covered with a regular array of microposts. It is shown that the classical Jeffreys' law, observed on flat solid, is deeply modified by the texture: 1) the film thickness does not follow anymore a scaling law, as a function of time; 2) below a critical thickness on the order of the pillar height, the film thickness drastically decreases; 3) at long time, a residual film remains trapped in the network of posts. All these facts are interpreted by considering the interaction between the "free film" flowing above the posts, and the "trapped film" inside the roughness. Beside a general description of the drainage of film on rough surfaces, our study shows that textures can be used to influence, or even block, the flow of liquid films on inclines.

The drainage of a liquid film (density ρ, viscosity η) coating an incline is an archetypal problem of interfacial hydrodynamics. Due to the film thinness, the flow reflects the boundary conditions at the solid/liquid and liquid/air interfaces, so that this problem is a model one for demonstrating anomalies at interfaces, such as generated by the presence of surfactants, textures or slip [1–4]. Let us start by the classical case of a thin film coating a flat vertical solid, as discussed in the early thirties by Jeffreys [5]. The film (of initial thickness h_o) thins because of gravity. In the lubrication approximation, the velocity profile can be calculated using a no-slip condition at the solid surface, and a no-stress condition at the liquid surface. This yields a parabolic velocity profile, and a flux Q per unit width: $Q = \rho g h^3/3\eta$, where h denotes the local film thickness. This quantity is *a priori* a function of time t and position x (x being the vertical coordinate with its origin at the top of the film). The function $h(x,\, t)$ is found by writing the flux conservation ($\partial Q/\partial x = -\partial h/\partial t$), which together with the expression for the flux Q leads to an evolution equation for the interface:

$$\frac{\partial h}{\partial t} = -\frac{\rho g h^2}{\eta}\,\frac{\partial h}{\partial x}. \tag{1}$$

By separating the variables x and t, Jeffreys showed that this equation admits two families of solution [5]: 1) a constant thickness $h \approx h_o$; 2) a parabolic profile ($h \sim \sqrt{x}$), which follows the Reynolds thinning law ($h \sim 1/\sqrt{t}$):

$$h(x,t) = \left(\frac{\eta x}{\rho g t}\right)^{1/2}. \tag{2}$$

Equation (2) expresses a balance between viscous resistance $\eta V/h^2$, and gravity ρg, where V denotes the mean velocity of the flow. If we write that V scales as x/t, we indeed recover eq. (2).

Both solutions of eq. (1) generally coexist, in two different regions: at the top of the film ($x = 0$), there is no liquid above so that the draining fluid is not replaced: the film thickness must then decrease with time in this region (eq. (2)). By contrast, one expects far from the top an invariance of the profile and the constant thickness $h \approx h_o$ should be observed. The transition between both solutions is expected when $h(x) \approx h_o$, that is, for $x \approx \rho g h_o^2 t/\eta$. The thinned parabolic region given by (2) thus propagates at the constant velocity $\rho g h_o^2/\eta$.

Our aim is to discuss how roughness at the solid surface modifies these simple laws, as it modifies spreading [6–10]. In order to be quantitative, we used as model rough substrates wafers covered with square arrays of cylindrical micro-posts (fig. 1). The dimensions of the texture

(a) E-mail: david.quere@espci.fr

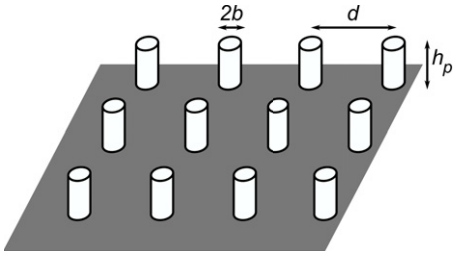

Fig. 1: Textured substrates used in this study: silicon wafers are etched, which leaves posts of height h_p, mutual distance d and radius b; h_p is between 1 and 35 μm, d is 10 or 20 μm, and b is 1.5 μm. The textures are "dilute": the ratio $\phi = \pi b^2/d^2$ between the top surface and the bottom one is much smaller than unity ($< 10\%$).

(height h_p between 1 to 35 μm, radius $b \approx 1.5\,\mu$m and mutual distance $d = 10$ or 20 μm) are well defined, owing to controlled etching [11]. The height in particular can be chosen with a precision of 100 nm, and passivation steps during etching allow us to generate pillars of large (>10) aspect ratio $h_p/2b$.

The textured substrate is plunged in a bath of silicone oil (of viscosity η between 10 and 350 mPa $\cdot$ s) from which it is withdrawn. The withdrawal velocity (1 to 10 mm/s) selects an initial uniform film thickness h_o between h_p and a few times h_p (typically 10 to 50 μm) [4,12,13]. Then, the plate is stopped and kept vertically, and the film thickness is measured as a function of time at a fixed position x below the top of the film. The measurement is performed by reflectometry: a probe illuminates the sample with a spot of white light (0.5 mm in diameter) and collects the reflected light. The frequency spectrum shows oscillations, due to the interferences arising from the presence of the film. The film thickness is deduced from this spectrum, with uncertainties smaller than 5%. We checked that the signal reflected by the wafer is not affected by the presence of micro-posts, whose surface concentration $\phi = \pi b^2/d^2$ remains modest, on the order of 5 to 10%.

We compare in fig. 2 the time evolution of the film thickness on surfaces either flat or textured. The initial thickness is equivalent in both experiments (about 40 μm), the oil is the same ($\eta = 19.5$ mPa $\cdot$ s), and the measurement is made at $x \approx 1$ cm below the top of the film.

Apart from the very beginning ($t < 10$ s), the drainage is found to be different in the two experiments. On a smooth solid (fig. 2a), the film thickness obeys Jeffreys' law: it first remains constant ($h \approx h_o \approx 45\,\mu$m), for about 10s— a duration in close agreement with the time $\eta x/\rho g h_o^2 \approx 10$ s deduced from eq. (2). Later, the film thickness decreases as $t^{-1/2}$, as expected from eq. (2) drawn with a solid line for $x = 12$ mm, a value comparable to the distance between the top of the film and the probe (about 1 cm). On the textured solid, the film also thins for $t > 10$ s, but the drainage is slower than on a flat solid, as indicated by Jeffreys' exponent $-1/2$ in the figure. However, at $t \sim 800$ s, the drainage suddenly accelerates, and the thickness

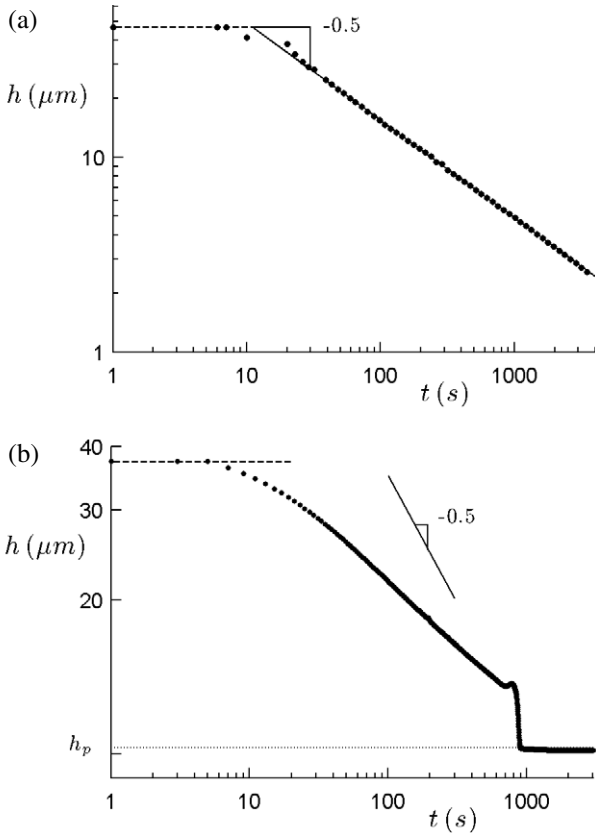

Fig. 2: Gravitational thinning of a viscous film on a vertical substrate, as a function of time. The film is made of silicone oil (viscosity $\eta = 19.5$ mPa $\cdot$ s and density $\rho = 970$ kg/m^3), and its thickness h is measured by reflectometry about 1 cm below the top of the film. (a) The substrate is a flat silicon wafer. The dashed line indicates the initial thickness $h = h_o$, and the solid line shows eq. (2) (Jeffreys' law), with $x = 12$ mm. (b) The substrate is a similar wafer, yet covered with a square array of microposts of height $h_p = 10.2\,\mu$m, diameter $2b = 3\,\mu$m and mutual distance $d = 10\,\mu$m. The solid line shows the slope $-1/2$, and the dotted line the pillar height $h = h_p$.

rapidly falls from 13 μm to 10.2 μm. This step-behavior happens when the film thickness approaches the pillar height, which it matches at longer time. This terminal regime is quite natural: at the texture scale, gravitational effects are much smaller than surface effects, so that a wetting liquid such as silicone oil remains trapped between the posts despite the action of gravity [8].

For characterizing the beginning of the drainage (until the step occurs), we plot in fig. 3 the thickness $h_f = h - h_p$ of the "free film" standing above the pillars. We again show in the graph the slope $-1/2$.

In this logarithmic representation, it is observed that the thickness of the free film does not follow a scaling law. In addition, its drainage can become quicker than on a flat solid —a consequence of the existence of liquid within the pillars, on which the free film somehow slips. It is indeed tempting to describe the influence of this underlying layer via a slip condition at the boundary between both films,

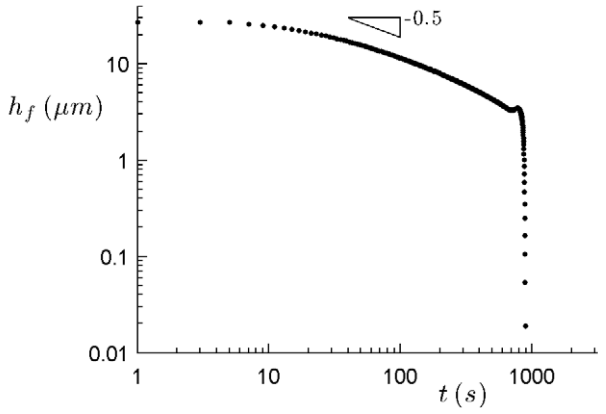

Fig. 3: Gravitational thinning of a viscous film on a vertical textured substrate, as a function of time. The data are the same as in fig. 2b, but we now show the time evolution of the thickness $h_f = h - h_p$ of the "free" film standing above the pillars of height h_p. We also indicate the slope $-1/2$.

as proposed by Beavers and Joseph for liquids flowing on saturated porous media [3]. We shall see later that a pure slip condition generates a $1/t$-behavior for the free film, which is not observed in fig. 3. Therefore we propose instead to describe this system as the superposition of two films, as sketched in fig. 4: a trapped film of thickness h_p with an effective viscosity $\alpha\eta > \eta$ (because the pillars increase the friction), and a free film of thickness h_f and viscosity η. Such a description recently allowed us to model the uptake of liquid by a textured substrate drawn out of a bath [13]. We also showed in [13] how α depends on the texture: since the friction in the trapped layer takes place on both the bottom surface and pillar walls, the viscous force scales as $\eta V/h_p^2 + \eta V/d^2$, larger by a factor $\alpha \sim 1 + h_p^2/d^2$ than the force $\eta V/h_p^2$ resisting the flow of a film of thickness h_p on a flat surface. Hence the geometrical ratio h_p/d fixes the effective viscosity $\alpha\eta$ of the trapped layer, which can be varied over a large interval.

In the lubrication approximation, we can calculate the velocity profile in both layers. The four associated boundary conditions are classically a no-slip condition at the solid surface ($y = 0$), a no-stress condition at the free surface ($y = h$) and the continuity of both the velocity and stress at the boundary between the two layers ($y = h_p$). Hence we get two parabolic profiles for the velocity, which can be written respectively: $u(y) = (\rho g/\alpha\eta)\ (y^2/2 - hy)$ for $y < h_p$ (trapped film); and $u(y) = (\rho g/\eta)\ (y^2/2 - hy + (1 - 1/\alpha)(h_p^2/2 + h_p h_f))$ for $y > h_p$ (free film). We deduce the total flux Q of liquid flowing downwards, expressed per unit length perpendicular to the plane of fig. 4:

$$Q = \frac{\rho g}{3\alpha\eta}(\alpha h_f^3 + 3h_f^2 h_p + 3h_f h_p^2 + h_p^3). \qquad (3)$$

Conservation of flux imposes $\partial Q/\partial x = -\partial h/\partial t = -\partial h_f/\partial t$, from which we obtain an evolution equation for

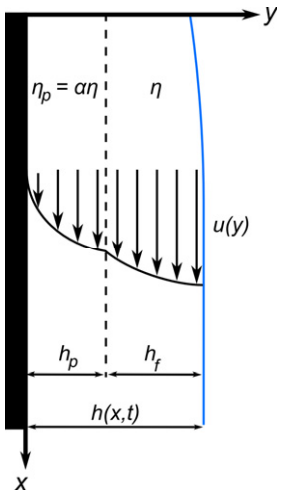

Fig. 4: (Colour on-line) In our model, we decompose the film of thickness h in two layers: 1) A layer trapped inside the pillars (of height h_p), treated as a film of viscosity $\alpha\eta$ larger than the liquid viscosity η; since the pillars increase the friction of the liquid, α has to depend on the geometry of the array of pillars. 2) A free layer of thickness h_f flowing above the previous one. In the lubrication approximation, the velocity $u(y)$ has a parabolic profile in each layer (see the text).

the (free) interface:

$$\frac{\partial h_f}{\partial t} = -\frac{\partial h_f}{\partial x}\frac{\rho g}{\alpha\eta}(\alpha h_f^2 + 2h_f h_p + h_p^2). \qquad (4)$$

For either $h_p \to 0$ or $\alpha \to \infty$ (in the latter limit, the posts are so dense that the trapped layer cannot move anymore, as if it were solid), we logically recover eq. (1). If the deposited film is thick enough ($h_f > h_p/\alpha$, always true in this study), the first term in the bracket is dominant at short time, so that we expect Jeffreys' solution for the free film (constant thickness first, then $h_f \sim (\eta x/\rho g t)^{1/2}$): the free film is so thick that textures do not influence its drainage. Later, the film gets thinner, and the second term in the bracket may become dominant. This term describes the flow of a free film on a substrate on which it slips, with a slip length $\lambda = h_p/\alpha$ and for $h_f > \lambda$. Considering this term alone, we obtain the corresponding drainage behavior:

$$h_f = \frac{\alpha\eta x}{2\rho g h_p t}. \qquad (5)$$

We indeed observe in fig. 3 an acceleration of the drainage as the film thins, but the scaling law expected from eq. (5) ($h_f \sim 1/t$) is clearly not obeyed. This can be understood: we would expect such a regime if the second term in bracket were larger than the two others, which implies $h_f > h_p$ and $h_f < h_p/\alpha$. Since α is by definition larger than unity, these two inequalities cannot be satisfied simultaneously, which implies that the essence of this problem cannot be captured by a simple slip condition at the boundary between the films. But eq. (4) also includes the flow inside the texture (third term in the brackets),

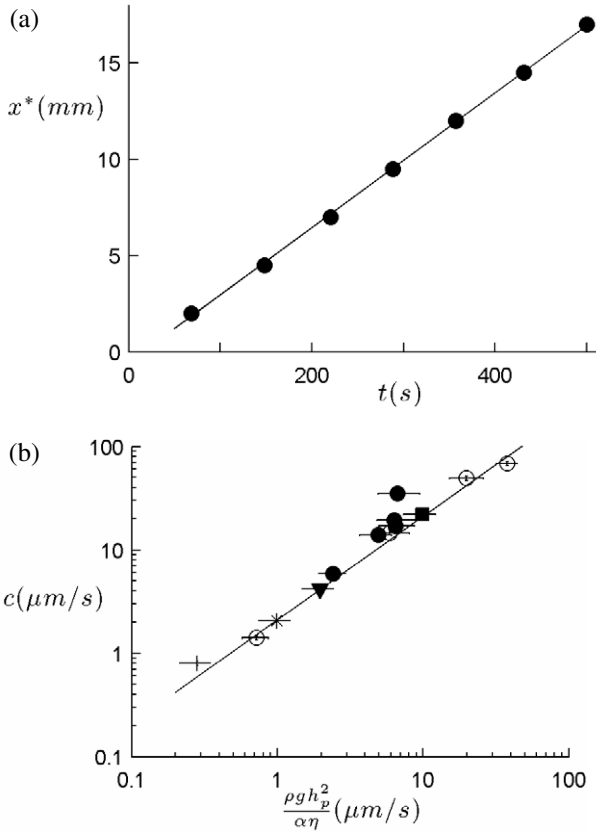

Fig. 5: (a) Time evolution of the position x^* of the step observed in figs. 2(b) and 3: the step moves downwards at a constant velocity $c = x^*/t$ (here $35\,\mu$m/s). (b) Step velocity c as a function of the velocity at which a film of height h_p falls inside the texture (eq. (6)). Both velocities are found to be comparable (the line has a slope 1). Full and empty symbols correspond to $p = 10$ and $p = 20\,\mu$m, respectively, and the symbols indicate different viscosities (square: $\eta = 9.7\,\mathrm{mPa\cdot s}$, circle: $\eta = 19\,\mathrm{mPa\cdot s}$, triangles: $\eta = 48\,\mathrm{mPa\cdot s}$, star: $\eta = 97\,\mathrm{mPa\cdot s}$, +: $\eta = 340\,\mathrm{mPa\cdot s}$).

which turns out to be a key fact for understanding what happens as the film thins ($h_f < h_p$). Then, this third term becomes dominant, so that eq. (4) becomes a convection equation $\partial h_f/\partial t = -(\rho g h_p^2/\alpha\eta)\partial h_f/\partial x$. The (free) liquid film gets entrained by the underlying film at a velocity c given by

$$c = \frac{\rho g h_p^2}{\alpha\eta}, \tag{6}$$

where both the pillar height and the factor α (itself a function of h_p) reflect the influence of the trapped layer. Hence the step in figs. 2b and 3 can be interpreted as the passage below the probe of the extremity of the free film entrained by the underlying layer: if we balance the viscous force $\alpha\eta V/h_p^2$ in this layer with gravity ρg, we indeed find $V = c$ (eq. (6)).

By displacing the probe along the vertical direction, we could follow the position x^* of the step as it moves downwards along the plate. As seen in fig. 5a, the step falls

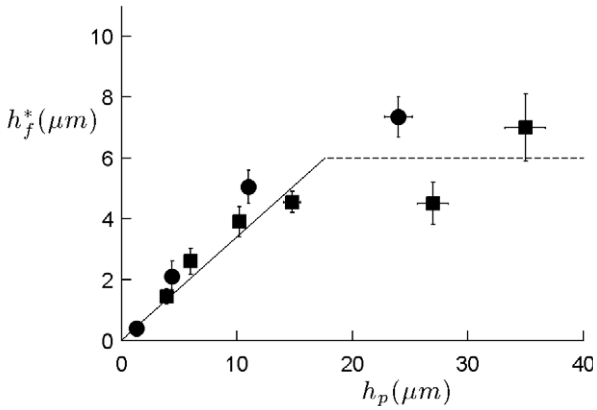

Fig. 6: Critical thickness h_f^* of the free film at the moment of the step, as a function of the pillar height. For small pillars, the critical thickness increases linearly with h_p. When the pillar height becomes comparable to the distance d between pillars, the critical height saturates. (Squares: $d = 10\,\mu$m, circles: $d = 20\,\mu$m.)

at a constant velocity c (in this example, $c \approx 35\,\mu$m/s); we measured this velocity for various samples ($d = 10$ or $20\,\mu$m, $h_p = 1.5$–$35\,\mu$m), and found that c depends on the solid texture, as shown in fig. 5b where it is plotted as a function of $\rho g h_p^2/\alpha\eta$, as suggested by eq. (6). In this expression, the numerical coefficient α was determined experimentally for each sample from withdrawal experiments [13]. In [13], it was also found to be captured by the formula $\alpha \approx 1 + 7.2 h_p^2/d^2$. In fig. 5b, the line shows a slope 1: eq. (6) is indeed obeyed.

This interpretation also allows us to predict the film thickness h_f^* at which the step occurs. As mentioned earlier, the third term then becomes dominant in the brackets of eq. (3), *i.e.* for $h_f < h_p/\sqrt{\alpha}$ and $h_f < h_p$. If α is on the order of unity (small and/or dilute pillars), these conditions become equivalent ($h_f < h_p$). If α is large, we saw that it varies as h_p^2/d^2, so that these conditions can be written $h_f < d$. Hence we expect h_f^* to vary as $\min(h_p, d)$, which can be checked: as seen in figs. 2b and 3, the value of h_f^* can be extracted quite clearly from the data. We plot in fig. 6 the variation of this "critical" thickness, as a function of the post height: it is first proportional to the pillar height h_p, before saturating when h_p becomes comparable to the spacing d. Uncertainties on h_f^* do not allow us to be very precise in this limit.

In summary, this study shows that the dynamics of drainage can be dramatically influenced by the presence of roughness at a solid surface. We considered as a model roughness disconnected bumps, which generates capillary trapping at long time, and flow between the structures before. The latter effect leads in particular to an acceleration of the drainage as the final residual thickness is approached. More generally, these findings suggest that drainage should be sensitive to the roughness design. In this study, the possibility for the liquid to flow between the pillars was found to be crucial. But other kinds of

roughness such as micro-holes (or micro honeycombs) at the surface do not permit a continuous flow below the free film, which should impact differently drainage. Hence microstructures at a solid surface do not only modify the kinetics of drainage; their design should also allow us to tune the nature of these kinetics.

* * *

We thank M. Reyssat for providing the textured samples.

REFERENCES

[1] Sonin A. A., Bonfillon A. and Langevin D., *Phys. Rev. Lett.*, **71** (1993) 2342.
[2] Scheid B. *et al.*, *EPL*, **90** (2010) 24002.
[3] Beavers G. S. and Joseph D. D., *J. Fluid Mech.*, **30** (1967) 197.
[4] Krechetnikov R. and Homsy G. M., *Phys. Fluids*, **17** (2005) 102108.
[5] Jeffreys H., *Proc. Cambridge Philos. Soc.*, **26** (1930) 204.
[6] Cazabat A. M. and Cohen-Stuart M. A. C., *J. Phys. Chem.*, **90** (1986) 5845.
[7] McHale G., Shirtcliffe N. J., Aqil S., Perry C. C. and Newton M. I., *Phys. Rev. Lett.*, **93** (2004) 036102.
[8] Ishino C., Reyssat M., Reyssat E., Okumura K. and Quéré D., *EPL*, **79** (2007) 56005.
[9] Courbin L., Denieul E., Dressaire E., Roper M., Ajdari A. and Stone H. A., *Nat. Mater.*, **6** (2007) 661.
[10] Savva N., Kalliadasis S. and Pavliotis G. A., *Phys. Rev. Lett.*, **104** (2010) 084501.
[11] Callies M., Chen Y., Marty F., Pépin A. and Quéré D., *Microelectron. Eng.*, **78-79** (2005) 100.
[12] Chen J. D., *J. Colloid Interface Sci.*, **109** (1986) 341.
[13] Seiwert J., Clanet C. and Quéré D., *J. Fluid Mech.*, **669** (2011) 55.